Detection of special nuclear material from delayed neutron emission induced by a dual-particle monoenergetic source

M. Mayer,[1,a)] J. Nattress,[2] and I. Jovanovic[2,b)]
[1]*Department of Mechanical and Nuclear Engineering, The Pennsylvania State University, University Park, Pennsylvania 16802, USA*
[2]*Department of Nuclear Engineering and Radiological Sciences, University of Michigan, Ann Arbor, Michigan 48109, USA*

(Received 12 May 2016; accepted 19 June 2016; published online 30 June 2016)

Detection of unique signatures of special nuclear materials is critical for their interdiction in a variety of nuclear security and nonproliferation scenarios. We report on the observation of delayed neutrons from fission of uranium induced in dual-particle active interrogation based on the $^{11}B(d,n\gamma)^{12}C$ nuclear reaction. Majority of the fissions are attributed to fast fission induced by the incident quasi-monoenergetic neutrons. A Li-doped glass–polymer composite scintillation neutron detector, which displays excellent neutron/γ discrimination at low energies, was used in the measurements, along with a recoil-based liquid scintillation detector. Time-dependent buildup and decay of delayed neutron emission from ^{238}U were measured between the interrogating beam pulses and after the interrogating beam was turned off, respectively. Characteristic buildup and decay time profiles were compared to the common parametrization into six delayed neutron groups, finding a good agreement between the measurement and nuclear data. This method is promising for detecting fissile and fissionable materials in cargo scanning applications and can be readily integrated with transmission radiography using low-energy nuclear reaction sources. *Published by AIP Publishing.* [http://dx.doi.org/10.1063/1.4955051]

The detection of special nuclear material (SNM) embedded in cargo during transit has been one of the long-standing challenges and areas of research in nuclear security.[1] It is widely accepted that active interrogation (AI)[2] is needed to address this problem, but the complexities that arise in development and use of AI methods are numerous. It is desirable to identify a suitable combination of AI probe particle source, radiation detectors, and measurement protocols that enable the observation of unique signature(s) of SNM with high signal-to-background ratio. Radiation dose to cargo has a prominent role in the selection of the AI probe.[3,4]

Emission of β-delayed neutrons that accompanies the fission process is a reliable signature that can indicate the presence of SNM.[5–13] A fission fragment (also called a delayed neutron precursor) undergoes β-decay into a daughter nuclide. The daughter nuclide can be produced in a highly excited state and subsequently emits a "delayed" neutron. It is a custom to categorize the delayed neutrons into groups based on the half-life of their precursors; the groups are characterized by their relative abundance and absolute group yield. These parameters depend on the nuclide and the type and energy of the particle used to induce fission, and have been measured for $^{235,238,233}U$, $^{239,240}Pu$, and ^{232}Th.[14,15] It has been shown that the differences in delayed neutron decay rates for short-lived neutron groups can be used to identify the isotopes from which the fission originated,[16] and it has been suggested that comprehensive exploitation of multiple signatures, including those originating from longer-lived delayed neutron groups, is desirable.[17]

Both high-energy photons and neutrons of various energies can be used to induce fission. In AI measurements, photon and/or neutron flux produced by the source is dominant while the beam is on. In AI systems based solely on high-energy photons, neutrons can be produced by photonuclear reactions[18] as well as by photofission.[19] If a repetitively pulsed AI beam is used, the buildup of delayed neutrons can be observed between the AI pulses.[20] Only a fraction of the time between pulses can be used for effective delayed neutron detection, since a significant background from prompt neutron die-away exists immediately after each AI pulse.[5] Once the AI beam is turned off, the remaining neutron flux is attributed to delayed neutron emission and the neutron background. Background neutrons originate from sources such as cosmic ray interactions, activation products, e.g., ^{17}N,[21] or from spontaneous fission of naturally occurring radionuclides. Although the rate of delayed γ ray emission is significantly higher than the rate of delayed neutron emission,[22] the γ ray background is high, the surrounding material is typically activated, and γ rays can be significantly self-attenuated or attenuated by high-Z shielding. Detectors with high energy resolution can be used to isolate delayed γ's from other γ background, but their high cost makes it difficult to implement the necessary large solid-angle coverage.

One challenging aspect of using the delayed neutron signature of SNM is the choice of radiation detectors. To date, moderated ^{3}He detectors were used to detect delayed neutrons,[23] but they are expensive, which can make the necessary instrumentation of a large solid angle impractical. Further, the moderated ^{3}He detectors do not provide spectroscopic capabilities, which make it more challenging to reject the high-energy neutron background, such as cosmogenic

[a)]Current address: Pacific Northwest National Laboratory, Richland, WA 99354, USA.
[b)]Electronic mail: ijov@umich.edu

neutrons and neutrons from spontaneous fission. Many of the current alternatives to ^{3}He have difficulty discriminating low energy neutrons in high γ fields.[24] The mean energy of delayed neutrons is approximately 0.5 MeV, making their detection using recoil-based detectors such as liquid scintillators significantly less efficient than that for prompt neutrons, since the threshold of such detectors must be set relatively high in the accompanying γ-ray field.

In this work, we demonstrate the combined use of a dual-particle AI source, neutron scintillation detectors readily scalable to large sizes, and methods of measurement and data interpretation for effective detection of SNM. First, we show that an AI source based on the ^{11}B(d,nγ)^{12}C nuclear reaction and suitable for dual-energy γ transmission radiography[13] can also induce a unique delayed neutron signature (buildup and decay) to confirm the presence of SNM. Second, we show the use of two types of spectroscopic neutron detectors for this task: a glass-polymer composite capture-gated detector,[25] which has high γ ray rejection capability for lower energy neutrons, and the EJ-309 liquid scintillation detector[26] with high sensitivity to higher-energy neutrons. Finally, we experimentally demonstrate a measurement and analysis protocol that reveals and integrates time-dependent delayed neutron buildup and decay signatures originating from longer-lived delayed neutron groups to infer the presence of SNM. We corroborate those experimental results by comparing the observed neutron emission rate with that predicted by nuclear data—specifically, the parametrization into six delayed neutron groups for fast fission of ^{238}U, finding good agreement with the measurement.

The measurements were performed at the Massachusetts Institute of Technology's (MIT) Bates Research and Engineering Center. The 3-MeV radio-frequency quadrupole (RFQ) accelerator was used to produce a deuteron beam. A natural boron accelerator target, consisting of ^{10}B (19.9%) and ^{11}B (80.1%), was inserted into the vacuum system of the accelerator and nitrogen gas was flowed across the accelerator target head for cooling during the experimental run. Lead and borated high-density polyethylene were placed around the accelerator target to restrict the emitted radiation to a beam. The accelerator was operated at a current of 20 μA and repetition rate of 300 Hz in three runs, each one lasting 2 min. Natural uranium and tungsten test objects were placed 1 m downstream from the boron target. Natural uranium consisted of rods (27.5 mm in diameter and 238.1 mm in height) encased in aluminum. The mass of each rod was approximately 1.9 kg, and a total of ten rods were used. Blocks of tungsten with varying shapes were assembled to construct a mass of tungsten approximately equal to the mass of natural uranium used in the experiment. More details on the experimental layout and the data acquisition are provided in the supplementary material.[27]

Two types of neutron detectors were placed on opposite sides of interrogated test objects outside of the AI fan-beam line. An EJ-309 liquid scintillator detector assembly (Eljen) was used, which included a Hamamatsu R7724 photomultiplier tube (PMT). The EJ-309 liquid is housed in a 53.9 mm diameter by 57.1 mm height aluminum chamber. The second detector is a custom-built composite scintillator comprised of Li-doped scintillating glass and scintillating polyvinyl-toluene (PVT),[25,28] with dimensions of 50.8 mm diameter by 50.5 mm height. The individual Li-glass pieces are in a square rod form factor oriented along the height of the PVT cylinder and placed in a pseudo-square array. This composite detector is a sub-scale prototype with an intrinsic efficiency of 0.33% for ^{252}Cf fission neutrons. The efficiency of the composite and liquid scintillation detector for delayed neutrons from fast fission of ^{238}U has been simulated, obtaining 1.2% and 1.4%, respectively.[27] The expected delayed neutron rate can be calculated from the microscopic cross sections for fission of ^{238}U by 15.1 MeV photons and fast neutrons,[29] approximating the incident fast neutron spectrum with 5-MeV monoenergetic neutrons. The fast neutron and 15.1-MeV photon production rates normalized to accelerator current were measured to be $1.3 \times 10^{9}\,\mathrm{s}^{-1}\,\mu\mathrm{A}^{-1}$ and $6.2 \times 10^{6}\,\mathrm{s}^{-1}\,\mu\mathrm{A}^{-1}$,[13] yielding the neutron and 15.1-MeV γ fluxes of approximately $2.1 \times 10^{5}\,\mathrm{cm}^{-2}\,\mathrm{s}^{-1}$ and $10^{3}\,\mathrm{cm}^{-2}\,\mathrm{s}^{-1}$ at the location at which test objects were placed, with the accelerator current set to 20 μA. The delayed neutron rate at the time the AI beam is turned off and is estimated to be $2.5 \times 10^{4}\,\mathrm{s}^{-1}$, with the majority of neutrons originating from fast-neutron-induced fission. The composite scintillation detector was positioned at a distance of 10 cm, while the EJ-309 detector was placed at a distance of 30 cm from the test object.

The first set of experimental data are shown in Figs. 1 and 2 as time-dependent running average of the detected neutron rate immediately after the AI beam is turned off. Fits

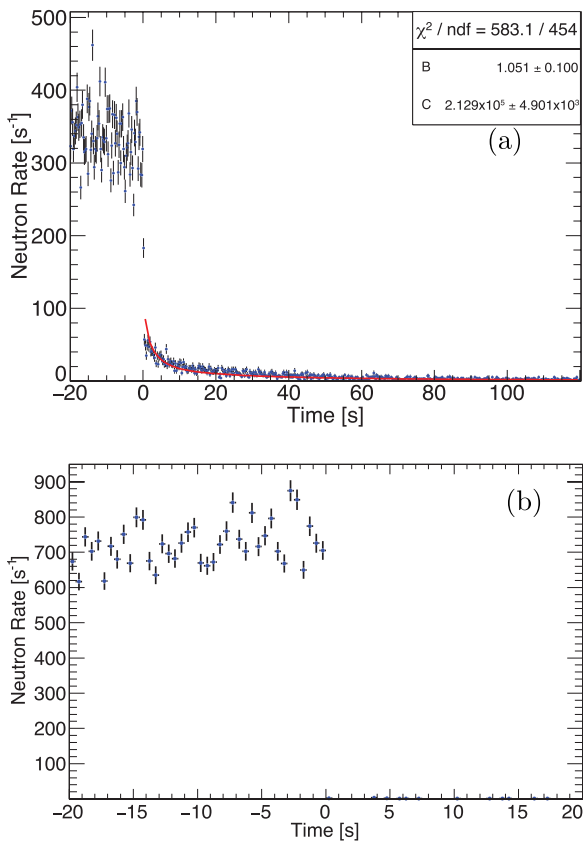

FIG. 1. β-delayed neutrons observed after the AI beam incident on (a) natural uranium and (b) tungsten after the beam is turned off ($t = 0$) for the composite scintillation detector. The fit to nuclear data is shown in red.

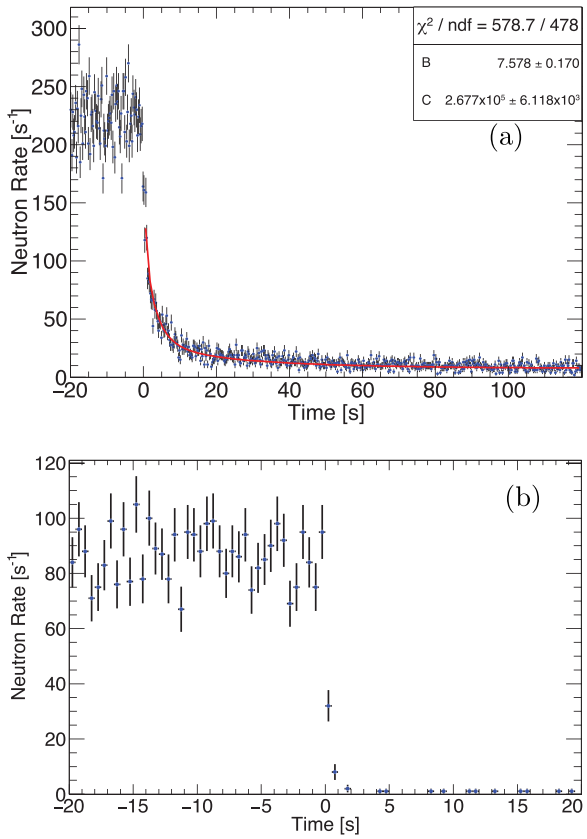

FIG. 2. β-delayed neutrons observed after the AI beam incident on (a) natural uranium and (b) tungsten after the beam is turned off ($t = 0$) for the EJ-309 liquid scintillation detector. The fit to nuclear data is shown in red.

to the measured delayed neutron rates have been calculated using a model based on contributions from six delayed neutron groups for fast neutron fission of ^{238}U, which also include the calculated detector efficiency for each neutron group. The model is formulated as follows:

$$R_d(t) = B + C\sum_{i=1}^{6} \epsilon_i Y_i(\exp(t_b/\tau_i) - 1)\exp(-t/\tau_i), \quad (1)$$

where $R_d(t)$ is the detected decaying delayed neutron rate, B is the constant neutron background, C is a scaling constant, index i is the group number, ϵ_i is the detector efficiency for group i, Y_i is the β-delayed neutron yield per fission for group i, and t_b is the period over which the AI beam was turned on. For the composite scintillation detector, the results for the natural uranium and tungsten test objects can be seen in Figs. 1(a) and 1(b), respectively. The equivalent results for the liquid scintillation detector are shown in Figs. 2(a) and 2(b).

A second set of delayed neutron signatures is obtained from analyzing the delayed neutron buildup between the accelerator pulses, starting with the time when the AI beam is turned on. The buildup data from both detectors for a uranium target were fitted to

$$R_b(t) = B + C\sum_{i=1}^{6} Y_i\epsilon_i(1 - \exp(-t/\tau_i)). \quad (2)$$

The tungsten data were fitted to a constant, in accordance with the expectation that there was no buildup of neutrons between the pulses. The results can be seen in Figs. 3 and 4 for the composite and the liquid scintillation detector, respectively. A buildup is present with the ^{238}U test object in the beam for both detectors. With both detectors, buildup is not observed with a control object composed of tungsten, which does not undergo nuclear fission. The efficiency of the composite capture-gated scintillation detector increases as the neutron energy is reduced, while maintaining the same ability to reject the γ background. As a result, the intrinsic detection efficiency for any neutrons that undergo scattering prior to reaching detector is further increased. Conversely, its efficiency is reduced for higher energy neutrons, such as those that can be produced by cosmic ray interaction with the surrounding material, and which would ultimately limit the sensitivity of the technique when larger detector coverage is used.

In conclusion, we demonstrated the detection of ^{238}U by observing the delayed neutron emission from its fission, which was induced by ^{11}B(d,n)^{12}C, a low-energy nuclear reaction source that produces both the abundant high-energy γ rays and fast neutrons. This AI source is suitable for γ imaging and can also supply a probe to confirm the presence of SNM.[13] It has been shown that detection can be performed not only using γ-blind detectors such as ^{3}He, but also using particle discriminating detectors readily scalable to achieve high coverage, including the EJ-309 liquid scintillator and a

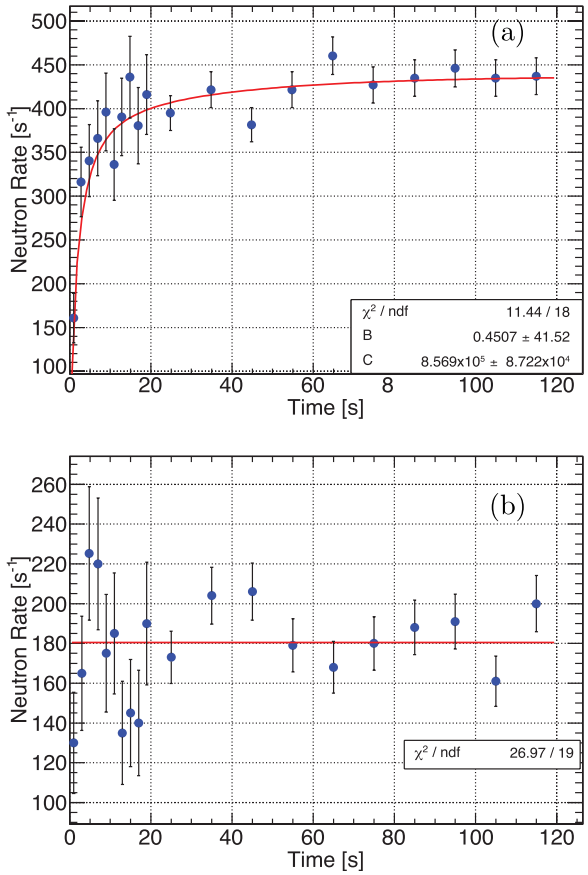

FIG. 3. β-delayed neutrons buildup observed with the composite scintillation detector during the AI beam incidence on (a) natural uranium and (b) tungsten. The beam is turned on at $t = 0$. The fit to nuclear data is shown in red.

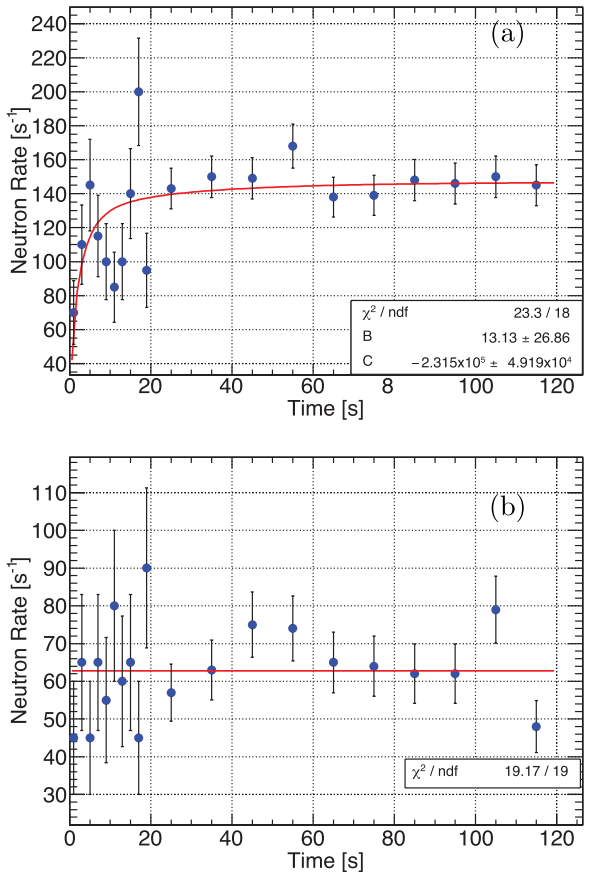

FIG. 4. β-delayed neutrons buildup observed with the EJ-309 detector during the AI beam incidence on (a) natural uranium and (b) tungsten. The beam is turned on at $t = 0$. The fit to nuclear data is shown in red.

specially developed composite glass-plastic scintillation detector. Those detectors also permit spectroscopic measurements, which will benefit rejection of higher energy neutrons that could be attributed to background, whose rate increases as the coverage and the absolute efficiency of the system increases.

As with any method, there are ways to circumvent this technique by using enough shielding. Fortuitously, the composite scintillation detector based on capture gating becomes more efficient as the energy of the neutron is reduced by shielding. This is a unique advantage that a capture-gated detector has over recoil-based detectors. The observation of both the buildup and decay of β-delayed neutrons from AI has been robustly achieved with this composite scintillation detector. The use of EJ-309 detector was more challenging due to its inability to accurately discriminate $\lesssim$1 MeV neutrons. Discrimination of different nuclides may also be possible using the buildup and decay time profile arising from long-lived delayed neutron groups, as previously shown with short-lived neutron groups.[16] We also note that both the capture-gated and recoil-based scintillation detectors could be used to reject high-energy neutron background and reduce the minimum detectable activity. With capture-gated detectors, it may also be possible to perform delayed neutron spectroscopy as an even further means for positive identification of a source,[15] although this may not be feasible in the presence of abundant shielding.

The work was supported by the National Science Foundation under Grant No. ECCS-1348366 and by the U.S. Department of Homeland Security under Grant Award No. 2014-DN-077-ARI078-02. The research of J.N. was performed under appointment to the Nuclear Nonproliferation International Safeguards Graduate Fellowship Program sponsored by the National Nuclear Security Administration's Next Generation Safeguards Initiative. The authors would like to thank P. Binns and H. Moazeni of MIT Bates Research and Engineering Center for help with operating the linear accelerator, to Z. Ounaies, A. Foster, A. Meddeb, and C. Trivelpiece of Pennsylvania State University for their contributions to the development of the neutron detector used in this work, to P. Rose and A. Erickson of Georgia Institute of Technology for their contributions to active interrogation experiments, and to Z. Hartwig of MIT for assistance with the ADAQ software.

[1]R. Kouzes, Am. Sci. **93**, 422 (2005).
[2]R. C. Runkle, D. L. Chichester, and S. J. Thompson, Nucl. Instrum. Methods Phys. Res., Sect. A **663**, 75 (2012).
[3]C. Moss, C. Hollas, G. McKinney, and W. Myers, IEEE Trans. Nucl. Sci. **53**, 2242 (2006).
[4]T. Taddeucci, R. Sheffield, T. Massey, D. Carter, J. O'Donnell, C. Brune, D. Ingram, D. Jacombs, and A. DiLullo, "Neutron and gamma-ray production with low-energy beams," Technical Report No. LA-UR-07-2724, Los Alamos National Laboratory, 2007.
[5]D. Chichester and E. Seabury, IEEE Trans. Nucl. Sci. **56**, 441 (2009).
[6]C. Moss, M. Brener, C. Hollas, and W. Myers, Nucl. Instrum. Methods Phys. Res., Sect. B **241**, 793 (2005).
[7]J. Lewis, R. Kelley, D. Murer, and K. Jordan, Appl. Phys. Lett. **105**, 014102 (2014).
[8]D. Norman, J. Jones, W. Yoon, K. Haskell, J. Sterbentz, J. Zabriskie, A. Hunt, F. Harmon, and M. Kinlaw, Nucl. Instrum. Methods Phys. Res., Sect. B **241**, 787 (2005).
[9]N. Bohr and J. Wheeler, Phys. Rev. **56**, 426 (1939).
[10]R. Roberts, L. Hafstad, R. Meyer, and P. Wang, Phys. Rev. **55**, 664 (1939).
[11]J. Church, D. Slaughter, S. Asztalos, P. Biltoft, M.-A. Descalle, J. Hall, T. Luu, D. Manatt, J. Mauger, E. Norman, D. Petersen, and S. Prussin, Nucl. Instrum. Methods Phys. Res., Sect. B **261**, 351 (2007).
[12]S. McConchie, P. Hausladen, J. Mihalczo, B. Blackburn, and D. Chichester, AIP Conf. Proc. **1099**, 643–646 (2009).
[13]P. B. Rose, A. S. Erickson, M. Mayer, J. Nattress, and I. Jovanovic, Sci. Rep. **6**, 24388 (2016).
[14]G. R. Keepin, T. F. Wimett, and R. K. Zeigler, Phys. Rev. **107**, 1044 (1957).
[15]G. Rudstam, Nucl. Sci. Eng. **80**, 238 (1982), see http://www.ans.org/pubs/journals/nse/a_21428.
[16]M. T. Kinlaw and A. W. Hunt, Appl. Phys. Lett. **86**, 254104 (2005).
[17]D. Chichester and E. Seabury, in *IEEE Nuclear Science Symposium Conference Record (NSS/MIC)* (2009), pp. 956–960.
[18]Y.-F. Wang, V. Balic, G. Gratta, A. Fassò, S. Roesler, and A. Ferrari, Phys. Rev. D **64**, 013012 (2001).
[19]D. H. Morse, A. J. Antolak, and B. L. Doyle, Nucl. Instrum. Methods Phys. Res., Sect. B **261**, 378 (2007).
[20]D. Chichester and E. Seabury, in Proceedings of the International Topical Meeting on Nuclear Research Applications and Utilization of Accelerators (International Atomic Energy Agency, Vienna, Austria, 2009).
[21]L. W. Alvarez, Phys. Rev. **75**, 1127 (1949).
[22]E. B. Norman, S. G. Prussin, R.-M. Larimer, H. Shugart, E. Browne, A. R. Smith, R. J. McDonald, H. Nitsche, P. Gupta, M. I. Frank *et al.*, Nucl. Instrum. Methods Phys. Res., Sect. A **521**, 608 (2004).
[23]D. Loaiza, Nucl. Instrum. Methods Phys. Res., Sect. A **422**, 43 (1999).
[24]L. Stevanato, D. Cester, G. Nebbia, and G. Viesti, Nucl. Instrum. Methods Phys. Res., Sect. A **690**, 96 (2012).
[25]M. Mayer, J. Nattress, V. Kukharev, A. Foster, A. Meddeb, C. Trivelpiece, Z. Ounaies, and I. Jovanovic, Nucl. Instrum. Methods Phys. Res., Sect. A **785**, 117 (2015).

[26]See http://www.eljentechnology.com/index.php/products/liquid-scintillators/73-ej-309 for "Eljen EJ-309 product description"; accessed 10 March, 2016.
[27]See supplementary material at http://dx.doi.org/10.1063/1.4955051 for additional information on the experimental setup and data analysis.
[28]M. Mayer, J. Nattress, C. Trivelpiece, and I. Jovanovic, Nucl. Instrum. Methods Phys. Res., Sect. A **784**, 168 (2015).
[29]M. Chadwick, M. Herman, P. Obložinský, M. Dunn, Y. Danon, A. Kahler, D. Smith, B. Pritychenko, G. Arbanas, R. Arcilla *et al*., Nucl. Data Sheets **112**, 2887 (2011).